



Study of triazolotriazepinon as a corrosion inhibitor in 1M hydrochloric acid

A. Harmaoui^a, H. Bourazmi^b, M. El Fal^{a*}, M. Boudalia^b, M. Tabyaoui^b, A. Guenbour^b,
A. Bellaouchou^b, Y. Ramli^c, E. M. Essassi^a

^a-Laboratoire de Chimie Organique Hétérocyclique, URAC 21, Pôle de Compétences Pharmacochimie,
Université Mohammed V, Faculté des Sciences, Av. Ibn Battouta, BP 1014 Rabat, Morocco.

^b-Laboratory of Materials, Nanotechnology and Environment, Faculty of Science, University of Mohamed-V-
Av. Ibn Battouta, BP 1014 Agdal-Rabat, Morocco.

^c-Medicinal Chemistry Laboratory, Faculty of Medicine and Pharmacy, Mohammed V, University-Rabat,
Morocco.

Received 20 Jan 2015, Revised 2015, Accepted 2015.

*Corresponding author. E-mail: elfal.mohammed@gmail.com

Abstract

The effect of triazolotriazepinon (TAT) on the corrosion of carbon steel (C35) in 1 M HCl is studied by the potentiodynamic polarization and impedance spectroscopy (EIS) measurements. The experimental results reveal that (TAT) has a good inhibiting effect on the metal tested in 1 M HCl solution. The protection efficiency increases with increasing inhibitor concentration to attain 84% at 10^{-3} M but decreased with temperature. Activation parameters and Gibbs free energy for the adsorption process were calculated and discussed. Potentiodynamic polarization curves indicated that the (TAT) derivative is a mixed-type inhibitor. Impedance measurements showed that the double layer capacitance decrease and charge-transfer resistance increase with increase in the inhibitor concentration. Adsorption of inhibitor on the steel surface in 1.0 M HCl follows the Langmuir isotherm model. The quantum chemical calculations is performed at the density functional theory (DFT) level using B3LYP functional with the 6-31G (d).

Keywords: Corrosion; Inhibitors; (TAT); Carbon Steel; DFT calculation.

Introduction

Acidic solutions are generally used in chemical and several industrial processes such as acid pickling, acid cleaning, acid descaling and oil well acidizing, which require the use of corrosion inhibitors [1 -3]. Iron and iron-based alloys of different grades are extensively used in numerous industrial and engineering applications, including construction and designs, where they are deployed in various service environments containing, acids, alkalis and salt solutions [4-6]. The use of inhibitors is one of the most practical methods of protecting against corrosion especially for materials in acidic media. Most of the well known inhibitors are organic compounds containing nitrogen, sulphur and/ or oxygen atoms. N-heterocyclic compounds are well qualified to play more protection for steel corrosion [6-8]. Many N-heterocyclic compounds such as derivatives of pyrazole [9-11], bipyrazole [12-14] triazole [15-17], tetrazole [18-20], imidazole [21-24], pyridine[25-28], pyrimidine [29] and pyridazine [30,31] have been reported as effective corrosion inhibitors for steel in acidic media. The heterocyclic compound containing nitrogen atoms can easily be protonated in acidic medium to exhibit good inhibitory action on the corrosion of metals in acidic solutions. The present study aimed to test new compound named triazolotriazepinon (TAT) on the corrosion of carbon steel C35 in 1M HCl solution. The study has been evaluated using potentiodynamic polarization, EIS and theoretical techniques. The inhibition efficiency of this compound at different temperatures and different concentrations elucidate the mechanism of the inhibition.

The relationships between the inhibition efficiency of the used compound in 1.0 M HCl and some quantum chemical parameters such as E_{HOMO} (highest occupied molecular orbital energy), E_{LUMO} (lowest unoccupied molecular orbital energy), the energy gap (ΔE_n) and the dipole moment(μ), has been also investigated by quantum chemical calculations.

2. Experimental Procedure

2.1. Materials

The chemical structure of the tested inhibitor, (TAT) is presented in Fig. 1. The material used in this study is a carbon steel (CS) (Euronorm: C35E carbon steel and US specification: SAE 1035) with a chemical composition (in wt%) of 0.370 % C, 0.230 % Si, 0.680 % Mn, 0.016 % S, 0.077 % Cr, 0.011 % Ti, 0.059 % Ni, 0.009 % Co, 0.160 % Cu and the remainder iron (Fe).

Prior to all measurements, the exposed area was mechanically abraded with 180, 320, 800, and 1200 grades of emery papers, rinsed with distilled water and degreased with acetone in an ultrasonic bath immersion for 5 min, washed again with distilled water and then dried at room temperature before use.

The aggressive solutions (1M HCl) were prepared by dilution of analytical reagent grade 37% HCl with distilled water.

The concentrations ranges of the inhibitor employed was 10^{-6} to 10^{-5} M. The product is synthesized by our group [32].

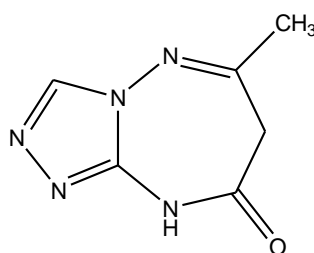
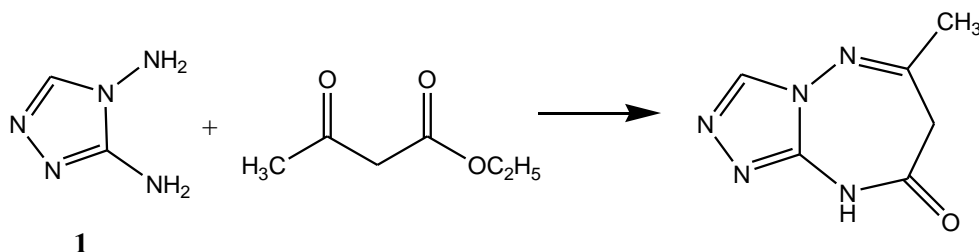


Fig. 1. Chemical structure of triazolotriazepinon (TAT)

3. Synthesis of the inhibitor

A mixture of 3,4-diamino-1,2,4- triazol **1** and the ethyl acetoacetate is refluxed for 3 hours. After cooling, the light yellow solid (70 % yield) obtained is characterized by ^1H NMR, ^{13}C NMR, and Mass Spectroscopy.



^1H NMR (DMSO): δ ppm: 2.28 (s, 3H, CH_3), 3.55 (s, 2H, CH_2), 8.71 (s, 1H, $\text{H}_{\text{Triazolo}}$).

^{13}C NMR (DMSO): δ ppm 24.93 (CH_3), 42.84 (CH_2), 141.41, 144.08, 164.78 (Cq), 164.99 (Cq, C=O).

HRMS (APPI) calcd for $\text{C}_6\text{H}_7\text{N}_7\text{O}$ (M^+) m/z : 165.

Anal. Calc of $\text{C}_6\text{H}_7\text{N}_7\text{O}$ C: 43.67, H: 4.48, N: 42.45. Found C: 43.38, H: 4.23, N: 42, 41.

2.3. Corrosion tests

2.3.1. Electrochemical measurements

The electrochemical measurements were carried out using system Voltalab PGZ 301 potentiostat piloted by a computer associated to VoltaMaster 4 software. A conventional three-electrode cylindrical Pyrex glass cell was used. The temperature is thermostatically controlled. The working electrode is a rectangular disk from carbon steel C35 with 1 cm^2 surface. A saturated calomel electrode (SCE) was used as a reference. The counter electrode (CE) was a platinum with the surface area of 1 cm^2 .

The working electrode (WE) was immersed in test solution at open circuit potential (OCP) for 30 min to be sufficient to attain a stable state. All electrochemical tests have been performed at 308 K.

The Electrochemical impedance spectroscopy (EIS) experiments were conducted in the frequency range between 100 kHz to 10 mHz at open circuit potential, with 10 points per decade, at rest potential after 30 min

of acid immersion, by applying 10 ac voltage peak-to-peak. All potentials were reported versus saturated calomel electrode (SCE). The impedance diagrams are given in the Nyquist representation. Experiments are repeated three times. The inhibition efficiency of the inhibitor was calculated from the charge transfer resistance values using the following equation [33]:

$$\eta_{EIS} = \frac{R_{ct(inh)} - R_{ct}}{R_{ct(inh)}} \times 100 \quad (1)$$

Where, R_{ct} and $R_{ct(inh)}$ are the charge transfer resistances in absence and presence of inhibitor respectively. The potential of potentiodynamic polarization curves was started from -800 to -300 mV/SCE, with a scan rate of 1 mV/s. The linear Tafel segments of anodic and cathodic curves were extrapolated to corrosion potential to obtain corrosion current densities (I_{corr}). The inhibition efficiency was evaluated from the measured I_{corr} values using the relationship [33] :

$$\eta_p(\%) = \frac{I_{corr} - I_{corr}^{inh}}{I_{corr}} \times 100 \quad (2)$$

Where I_{corr} and I_{corr}^{inh} represent corrosion current density values without and with inhibitor, respectively .

3. Results and discussion

3.1. Corrosion inhibition evaluation

3.1.1 Tafel polarization study

Potentiodynamic polarization measurements were carried out in order to gain knowledge concerning the kinetics of the anodic and cathodic reactions. Typical potentiodynamic polarization curves of the mild steel in 1 M HCl solutions without and with addition of different concentrations of the triazolotriazepinon (TAT) are presented in Fig.2. Electro chemical kinetic parameters (corrosion potential (E_{corr}), corrosion current density (I_{corr}), cathodic Tafel slope (β_c) and anodic Tafel slope (β_a)), determined from these experiments by extrapolation method, are regrouped in Table .1.

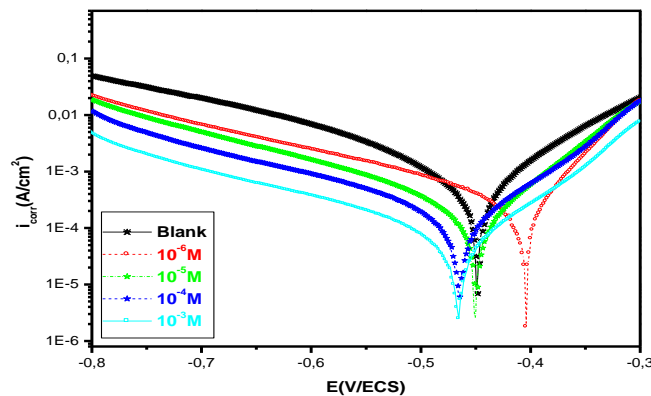


Fig .2.Tafel polarization curves for the corrosion of carbon steel C35 in 1 M hydrochloric acid containing different concentrations of the product at 308 K.

Anodic and cathodic polarization curves were obtained for carbon steel C35 in 1 M HCl solutions without and with different concentrations of triazolotriazepinon (TAT). The corrosion kinetic parameters derived from these curves (corrosion potential (E_{corr}), Tafel slopes (β_a , β_c), corrosion current density (I_{corr}) and degree of surface coverage (Θ), are given in Table.1. It is clear that the addition of triazolotriazepinon (TAT) reduce markedly the corrosion current density but slightly affect the values of (E_{corr}) indicating that it could act as pickling inhibitor [34]. The inhibition efficiency ($\eta_p\%$) increases with inhibitor concentration reaching 87% at 10^{-3} M. This behavior reflects its ability to inhibit the corrosion of carbon steel C35 in 1M HCl solution. The values of β_c change slightly in the presence of triazolotriazepinon (TAT). These results

indicate that the presence of (TAT) inhibit both the hydrogen evolution and anodic dissolution reactions, and their inhibiting action occurs only by simple blocking of the available surface areas [35-37]. Moves the corrosion potential to more negative values, as seen from the Fig. 2, indicates that (TAT) can be defined as a mixed-type inhibitor with predominance of the cathodic one [38–40].

Table .1. Polarization parameters for carbon steel C35 in 1 M HCl in the presence and absence of (TAT) at 308 K .

Concentration (g/L)	$-E_{\text{corr}}$ (mV. Vs. Ag/AgCl)	$-\beta_c$ (mV dec ⁻¹)	β_a (mV dec ⁻¹)	I_{corr} ($\mu\text{A cm}^{-2}$)	E_p (%)	Θ
blank	-451	116	98	325	-	-
10^{-6}	-403	111	49	108	66,7	0.667
10^{-5}	-450	97	66	88	77,5	0.775
10^{-4}	-445	105	79	60	81,5	0.815
10^{-3}	-465	95	73	41	87	0.87

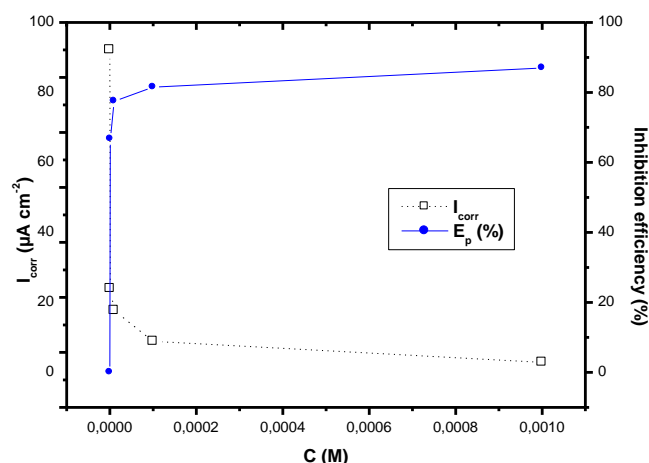


Fig.3. Variation of corrosion current density and inhibition efficiency of carbon steel C35 in 1M HCl containing various concentrations of (TAT).

3.4. Electrochemical Impedance Spectroscopy (EIS)

Impedance measurements of carbon steel C35 in 1 M HCl in the absence and the presence of the inhibitor at different concentrations plotted at open circuit potential (E_{corr}) at 308 K after 30 min are given in Fig. 2. It is clear that, from Fig. 4, the impedance diagrams consists of a large capacitive loop. The EIS study indicated that the capacitive loop is related to the charge transfer process of the metal corrosion and the double-layer behavior. The diameter of the capacitive loop in the presence of (TAT) is larger than that in the blank solution, and increases with the inhibitor concentration. Moreover, the highest inhibitor concentration of (TAT) (10^{-3} M) gives rise to much larger diameter of the capacitive loop than other for lower concentrations of (TAT) (Fig. 4). In fact, the presence of (TAT) increase the value of charge transfer resistance (R_{ct}) in acidic solution [41]. The diameter of the capacitive loop in the presence of (TAT) is larger than that in the blank solution, and increases with increasing of the inhibitor concentration. The EIS results of these capacitive loops are simulated by the equivalent circuit exposed in Fig.5. to purify electric models that could verify or rule out mechanistic models and permit the calculation of numerical values corresponding to the physical and/or chemical properties of the electrochemical system under investigation [42].

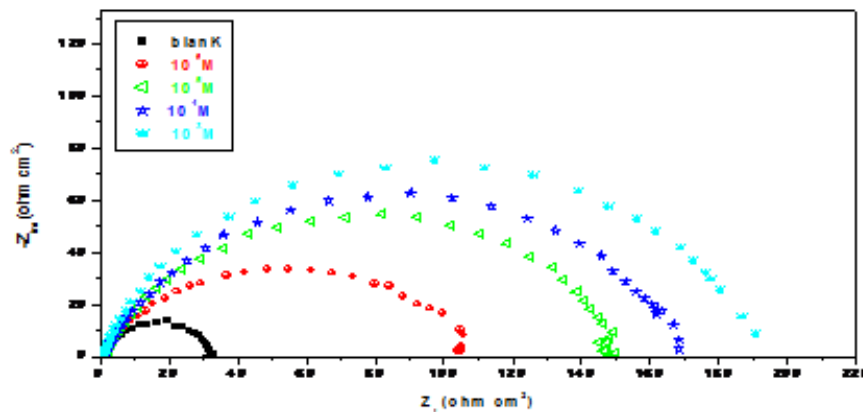


Fig.4. Nyquist plots of carbon steel C35 in 1 M HCl without and with different concentrations of (TAT) at 308 K.

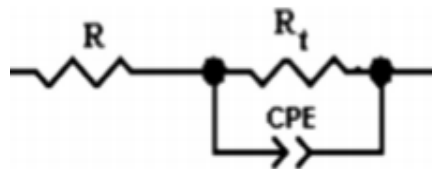


Fig.5. the equivalent circuit of the impedance spectra obtained for (TAT) at 308 K.

The impedance parameters derived from these studies using Z -view software are regrouped in Table 2. The values of charge transfer resistance (R_{ct}) that increased with inhibitor concentrations may suggest the formation of a protective film on the electrode/solution interface [41-43].

Table .2. Impedance parameters for corrosion of carbon steel C35 in 1M HCl without and with different concentrations of (TAT) at 308K.

Concentration (mol/L)	$R_{ct}(\Omega \text{ cm}^2)$	n	$10^4 Q (\text{S}^n / \Omega \text{ cm}^2)$	$C_{dl} (\mu\text{F cm}^{-2})$	$E_{EIS} (\%)$
Blank	31	0.79	0.88	212	-
10^{-6}	103	0.80	0.5	77	69.9
10^{-5}	145	0.81	0.39	58	78.6
10^{-4}	167.2	0.82	0.34	50	81
10^{-3}	192	0.86	0.32	48	84

The values of surface inhomogeneity coefficient (n) is an empirical exponent $0 \leq n \leq 1$ which measures the deviation from the ideal capacitive behavior [44] this number decrease with increasing of the inhibitor concentration. The value of capacitance (C_{dl}) can be calculated from CPE (Q) and a resistor (R_{ct}), using the following relation [45,46]:

$$C_{dl} = (Q \cdot R_{ct}^{1-n})^{1/n} \quad (3)$$

The constant phase element, CPE, is introduced in the circuit instead of a pure double layer capacitor in order to take into account the electrode surface heterogeneity resulting from, adsorption of inhibitors, formation of porous layers [47, 48]. The inhibition efficiency increase with increasing inhibitor concentration may be due to the elevation adsorption of this compound on the carbon steel C35 surface. The inhibition efficiency value calculated from EIS data is in good agreement with those obtained from electrochemical polarization method.

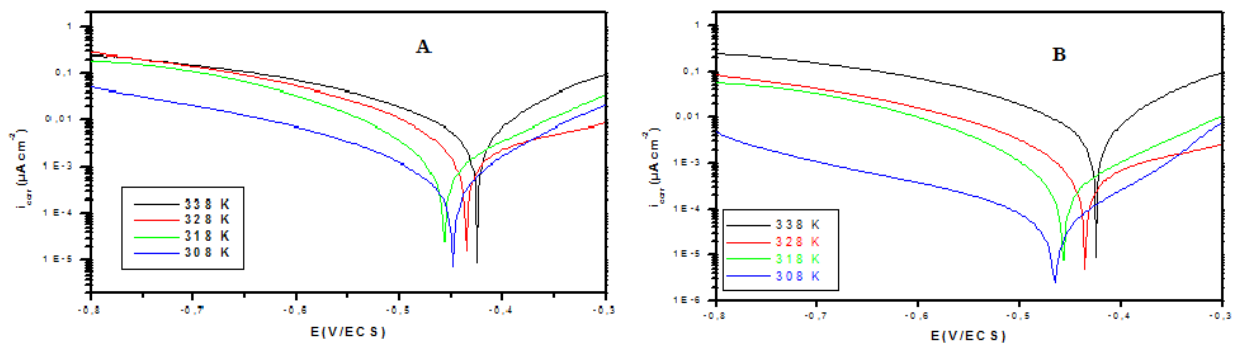


Fig.6. Tafel polarization curves for the corrosion of carbon steel at different temperatures (A) in 1M HCl and (B) in 1M HCl + 10⁻³M of (TAT)

Table.3. the influence of temperature on the electrochemical parameters for carbon steel electrode immersed in 1M HCL and in 1M HCl + 10⁻³ M of (TAT)

T(K)	Concentration (g/L)	-E _{corr} (mV. Vs. Ag/AgCl)	-β _c (mV dec ⁻¹)	β _a (mV dec ⁻¹)	I _{corr} (μA cm ⁻²)	E _p (%)
308	blank	-451	116	98	325	-
318		-461	42	38.3	417	-
328		-439	41	43.2	677	-
338		-429	130	88	1720	-
308	10 ⁻³	-465	95	73	41	87
318		-494	113.6	81.1	68	83.6
328		-469	97.9	66.9	140	79.3
338		-473	-120.2	83.4	658	62

3.5 Effect of temperature

The effect of the temperature on the inhibition efficiencies of (TAT) was also studied by polarization measurements in the absence and presence of 10⁻³ M of the inhibitor (TAT). The carbon steel is immersed during 30 min for each temperature (308 to 338K) as shown in Table 5. The various corrosion parameters obtained are listed in Table 3. The data obtained suggest that the I_{corr} values is more pronounced in both uninhibited and inhibited solutions and the value of inhibition efficiency decreases slightly with the rise of temperature. This data can be interpreted that, the inhibitor acts by adsorbing onto the metal surface, and an increase in the temperature causes desorption of some adsorbed inhibitor molecules, leading to a decrease in the inhibition efficiency, and hence to the decrease of surface coverage degree [49]. Activation parameters such as the activation energy, E_a, the enthalpy of activation, ΔH_a^{*}, and the entropy of activation ΔS_a^{*}, for both corrosion medium, with and without inhibitor of carbon steel in 1 M HCl in the absence and presence of optimum concentration of (TAT) were obtained from an Arrhenius-type plot (Eq. (4)) and the transition state (Eq. (5)) [50, 51] :

$$I_{corr} = A \exp\left(\frac{-E_a}{RT}\right) \quad (4)$$

Where I_{corr} is the corrosion current density, A the Arrhenius constant, E_a the activation energy, and R the universal gas constant.

$$I_{corr} = \frac{RT}{N_A h} \exp\left(\frac{\Delta S_a^*}{R}\right) \exp\left[-\frac{\Delta H_a^*}{RT}\right] \quad (6)$$

where h is Planck's constant, N is Avogadro's number, ΔS_a^{*} is the entropy of activation and ΔH_a^{*} is the enthalpy of activation.

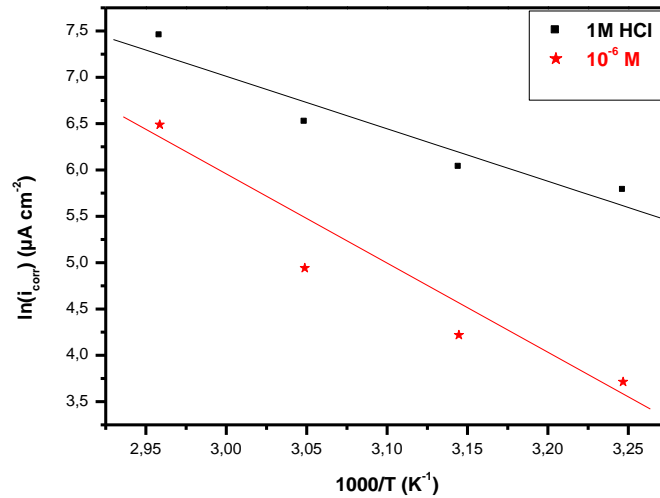


Fig. 7. Arrhenius plots of $\text{Ln}(I_{\text{corr}})$ versus $1000/T$ at 10^{-3} M concentrations of (TAT)

The plot of $\text{Ln}(I_{\text{corr}})$ vs. $1000/T$ and $\text{Ln}(I_{\text{corr}}/T)$ vs. $1000/T$ give straight lines with slopes of $-E_a/R$ and $-\Delta H_a^*/R$, respectively. The intercepts were A and $[\text{Ln}(R/Nh) + (\Delta S_a^*/R)]$ for the Arrhenius and transition state equations, respectively. Fig. 4 and Fig.5 represent the data plots of $\text{Ln}(I_{\text{corr}})$ vs. $1000/T$ and $\text{Ln}(I_{\text{corr}}/T)$ vs. $1000/T$ in the absence and the presence of 10^{-3} M concentration of (TAT). The calculated values of the activation energy E_a , the enthalpy of activation ΔH_a^* and the entropy of activation ΔS_a^* are summarized in Table 4.

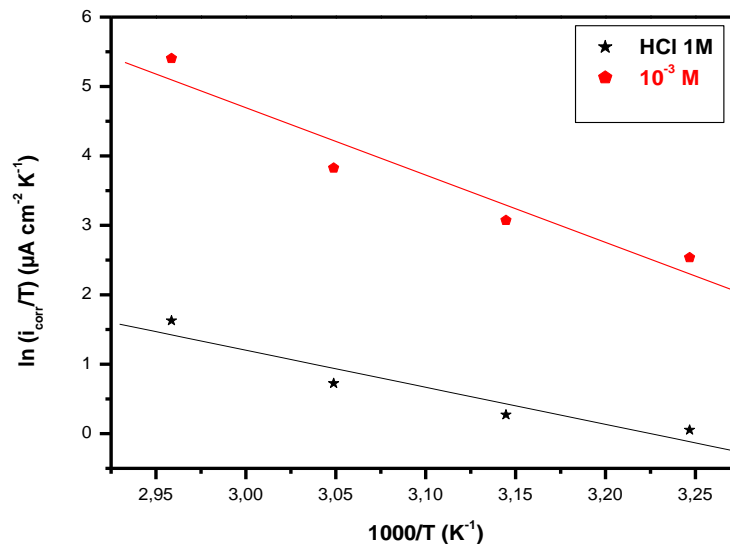


Fig. 8. Variation of $\text{Ln}(I_{\text{corr}}/T)$ versus $1000/T$ at various 10^{-3} M concentrations of (TAT).

The results given in table 2 show that, the E_a increased with inhibitor concentration of (TAT) than that of the uninhibited solution. This result is agree with a physical adsorption (electrostatic) in the first stage [52]. The activation energy rose with increasing inhibitor concentration, suggesting strong adsorption of inhibitor molecules at the metal surface. The increase in the activation energy was due to the corrosion reaction mechanism in which charge transfer was blocked by the adsorption of (TAT) molecules on the carbon steel surface [53].

Table.4. Corrosion Kinetic parameters for carbon steel in 1M HCl in absence and presence of 10^{-2} M of (TAT).

Inhibitor	E_a (KJ mol ⁻¹)	ΔH_a^* (KJ mol ⁻¹)	ΔS_a (J mol ⁻¹ K ⁻¹)	$E_a - \Delta H_a^*$
Blank	44.3	41.7	-48	2.6
TAT	77.31	74.66	88.79	2.65

The positive sign of ΔH_a^* implies that the carbon steel dissolution is an endothermic process which is in a good agreement with the observed increasing corrosion rate with increasing temperature. Moreover the value of ΔH_a^* increased in the presence of inhibitor than the uninhibited solution, indicating that the energy barrier for the corrosion reaction increased in the presence of inhibitor without changing the dissolution mechanism [54]. The entropy of activation (ΔS_a^*) shows two distinguished characteristics. In uninhibited corrosion process, the negative value of ΔS_a is typical of an association-based formation of the activated complex in the rate determining step of the reaction mechanism [55]. While the increase and positive sign of ΔS_a in the presence of (TAT) indicates the formation of an ordered layer onto the metal surface [56] and accounts for the disorder occurring during the formation of the activated complex [57].

3.6. Isotherme adsorption

From the impedance data, it is clear that the essential step in the inhibition mechanism is the adsorption of the inhibitor of (TAT) on the carbon steel surface [58]; therefore the observed decrease in double-layer capacitance C_{dl} result from improved adsorption of the inhibitor of (TAT) on the carbon steel surface. To describe the adsorption of the inhibitor on the steel surface, several adsorption isotherms were tested, including Freundlich, Temkin, Frumkin, Bockris–Swinkels, Flory–Huggin and Langmuir isotherms. However, the best agreement was obtained using the Langmuir adsorption isothermal equation as follow:

$$\frac{C}{\theta} = \frac{1}{K_{ads}} + C \quad (7)$$

where K_{ads} is the adsorptive equilibrium constant, C is the concentration of the additives and θ is the surface coverage. The Surface coverage values for (TAT) inhibitor as determined by the polarisation measurements for various concentrations of the inhibitors are reported in Table 2. As shown in Fig. 7, plotting C vs. C/θ results in a linear correlation. The strong correlation ($R^2 > 0.99$) suggests that the adsorption of inhibitor on the C35 surface obeye this isotherm. The adsorptive equilibrium constant (K_{ads}) is related to the standard adsorption free energy (ΔG_a^*) obtained according to [54-56]:

$$K_{ads} = \left(\frac{1}{C_{solvent}} \right) \exp\left(\frac{-\Delta G_a^*}{RT} \right) \quad (8)$$

where $C_{solvent}$ is the concentration of water in solution, R is the gas constant (8.314 J K⁻¹mol⁻¹), T is the absolute temperature (K), and the value of 55.5 is the concentration of water in the solution in mol/L [55].

Table.5. Thermodynamic parameters for the adsorption of (TAT) on the carbon steel in 1M HCl at 308K.

inhibitor	R^2	Slope	K_{ads} (M ⁻¹)	ΔG_{ads} (KJ mol ⁻¹)
(TAT)	0.999	1.146	3×10^5	-20.6

Generally, values of ΔG_{ads} around -20.6 kJ mol⁻¹ or lower are consistent with the electrostatic interaction between charged organic molecules and the charged metal surface (physisorption); those around -40 kJ mol⁻¹ or higher involve charge sharing or transfer from the organic molecules to the metal surface to form a coordinate type of bond (chemisorptions) [56,57]. Table 7 shows the values of ΔG_{ads} are in the range from 20 to 40 kJ mol⁻¹, probably means that both physical adsorption and chemical adsorption (mixed adsorption) would take place.

From Eq. (8), ΔG_a^* was calculated as -20.6 kJ mol⁻¹ for (TAT) inhibitor. The negative value of standard free energy of adsorption indicates spontaneous adsorption of our molecule on mild steel surface and also the

strong interaction between inhibitor molecule and the metal surface [57-65]. The value of ΔG^*_{ads} in our measurement is $-20.6 \text{ kJ mol}^{-1}$ for it suggested that the adsorption involves the physisorption interactions.

4. Quantum chemical calculations

Among the quantum chemical methods for the assessment of corrosion inhibitors, the functional theory of density, DFT has shown significant promise [64] and seems to be enough to notice changes in the electronic structure responsible of the inhibitory action. To explore the theoretical and experimental consistency, quantum chemical calculations were performed with full geometry optimizations using Gaussian-03 program [65]. The geometry of the molecules was optimized by the functional theory of density (DFT). Recently, the functional theory of density (DFT) was used to analyze the characteristics of the open mechanism of the inhibitor and to describe the structural nature of the inhibitor in the corrosion process [66, 67]. Furthermore, DFT is considered as a very useful technique for probing the inhibitor / surface of interaction and to analyze the experimental data. The results of the optimization of the geometry for compound (TAT) are presented in Table 5.

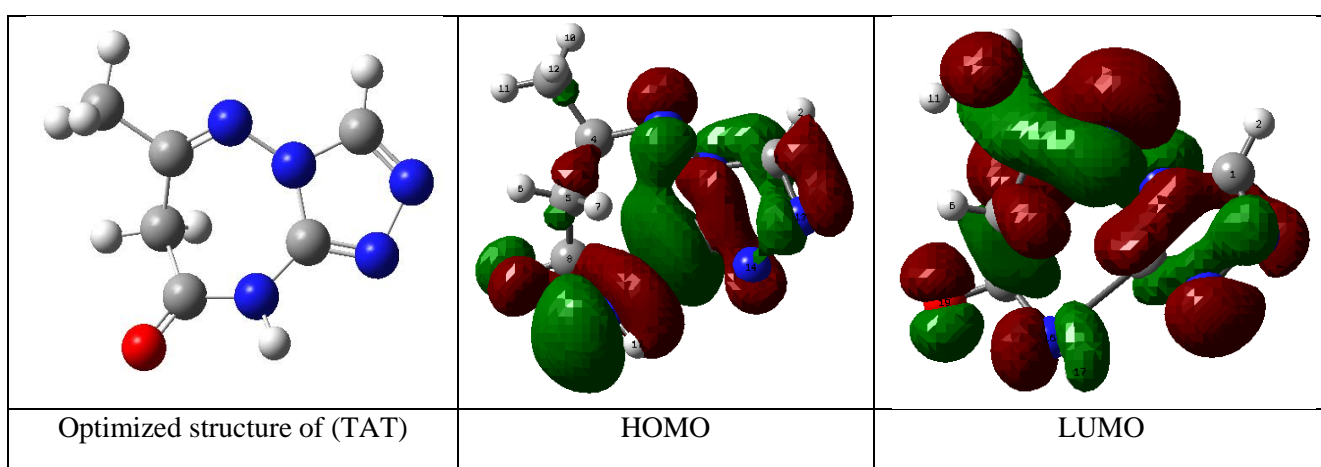


Table.6. Frontier molecular orbital density distributions of the (TAT).

Table.7. Calculated Quantum Chemical Parameters of the (TAT).

E_{HOMO} (eV)	E_{LUMO} (eV)	ΔE gap (eV)	μ (debye)	TE (eV)
-0.242	-0.174	0.068	4.760	-1454.400

We can see that the density of electrons from the HOMO of location in the molecule (TAT) is mainly distributed near the nitrogen (N) and oxygen (= O) atoms and also on ring triazolotriazepinon indicating that, they are the preferred sites for adsorption, while the density of LUMO is distributed around the entire molecule. The value of E_{HOMO} (-0.242 eV) should show a tendency of the molecule to donate electrons to the appropriate acceptor molecules with low energy and empty molecular orbital, while the value of E_{LUMO} (-0.174 eV) indicates the ability of the molecule to accept electrons. Therefore, the value of ΔE_{gap} provides a measure of the stability of the complex formed on the surface of the metal, the total energy of the triazolotriazepinon equals -1454.400 eV. This result indicated that triazolotriazepinon is favorably adsorbed by the active centres of adsorption. Lower values of the dipole moment (μ) of promote the accumulation of inhibitor in the surface layer and therefore a more efficient inhibition [68].

Conclusion

The (TAT) is a good inhibitor for corrosion of C35 in 1.0 M HCl solution. The inhibition efficiency increased markedly with the inhibitor concentration and reached 84 % but decrease at higher temperature. The inhibition action is performed via adsorption of the (TAT) constituents on C35 surface. The adsorption process is spontaneous and follows Langmuir adsorption isotherm. Activation energy decreases with addition of inhibitor. The calculated quantum chemical parameters such as HOMO–LUMO gap (ΔE), E_{HOMO} , E_{LUMO} , dipole moment (μ) and total energy (TE) were found to give good reasonably correlation with the efficiency of corrosion inhibition.

Référence

1. G. TrabANELLI, in: F. Mansfeld (Ed.), *Corrosion Inhibitors, Corrosion Mechanisms*, Marcel Dekker, Inc., New York, 1986, p. 119.
2. I.L. Rozenfeld, in: *Corrosion Inhibitors*, McGraw–Hill Inc., 1981, pp. 97–138.
3. G.S. Gradner, in: C. Nathan (Ed.), *Inhibitors in Acid Systems, Corrosion Inhibitors*, National Association of Corrosion Engineers, Houston, TX, 1973, p. 156.
4. A. Anejjar, A. Zarrouk, R. Salghi, D. Ben Hmamou, H. Zarrok, S. S. Al-Deyab, M. Bouachrine, B. Hammouti, N. Benchat. *Int. J. Electrochem. Sci.*, 8 (2013) 5961 - 5979
5. A. El Bribri, M. Tabyaoui, B. Tabyaoui, H. El Attari, F. Bentiss, *Materials Chemistry and Physics* 141 (2013) 240-247.
6. El Bribri A., Tabyaoui M., El Attari H., Boumhara K., Siniti M., Tabyaoui B., *J. Mat. Environ. Sci.* 2 (2011) 156-165.
7. M. Boudalia, A. Guenbour, A. Bellaouchou, R. M. Fernandez-Domene, and J. Garcia-Antonal *J. Inter Journal of Corros.*, 2013 (2013)9.
8. E.E. Foad El Sherbini, *Mater. Chem. Phys.*, 60 (1999) 286.
9. W.W. Frenier, F.B. Growcock and V.R. Lopp, *Corrosion.*, 44 (1988) 590.
10. M.A. Quraishi and D. Jamal, *Corrosion.*, 56 (2000) 156.
11. M. Benabdellah, A. Yahyi, A. Dafali, A. Aouniti, B. Hammouti and A. Ettouhami, *Arab. J. Chem.*, 4 (2011) 343.
12. M. Elayyachy, B. Hammouti, A. El Idrissi and A. Aouniti, *Port. Electrochim. Acta.*, 29 (2011) 57.
13. J.M. Sykes, *Br. Corros. J.*, 25 (1990) 175.
14. P. Chatterjee, M.K. Banerjee and K.P. Mukherjee, *Indian J. Technol.*, 29 (1991) 191.
15. J.M. Bockris, and B. Yang, *J. Electrochem. Soc.*, 138 (1991) 2237.
16. A. Zarrouk, I. Warad, B. Hammouti, A. Dafali, S.S. Al-Deyab and N. Benchat, *Int. J. Electrochem. Sci.*, 5 (2010) 1516.
17. D. A. Vermilyea, in, *First International Congress; Metal Corrosion; Butterworths; London; 1962*, p 62 .
18. F. Bentiss, M. Traisnel, N. Chaibi, B. Mernari, H. Vezin and M. Lagrenee, *Corros. Sci.*, 44 (2002) 2271 .
19. I.El Ouali, B. Hammouti, A. Aouniti, Y. Ramli, M. Azougagh, E.M., Essassi and M. Bouachrine, *J. Mater. Environ. Sci.*, 1 (2010) 1.
20. K.F. Khaled, N.S. Abdelshafi, A. El-Maghraby and N. Al-Mobarak, *J. Mater. Environ. Sci.*, 2 (2011) 166.
21. J. Uhrea and K. Aramaki, *J. Electrochem. Soc.*, 138 (1991) 3245.
22. S. Kertit and B. Hammouti, *Appl. Surf. Sci.*, 93 (1996) 59.
23. A. Chetouani, B. Hammouti, A. Aouniti, N. Benchat and T. Benhadda, *Prog. Org. Coat.*, 45 (2002) 373.
24. K. Bekkouch, A. Aouniti, B. Hammouti, S. Kertit, *J. Chim. Phys.*, 96 (1999) 838.
25. S. Kertit, B. Hammouti, M. Taleb and M.; Brighli, *Bull. Electrochem.*, 13 (1997) 241.
26. M. Bouklah, N. Benchat, A. Aouniti, B. Hammouti, M. Benkaddour, M. Lagrenee, H. Vezin and F. Bentiss, *Prog. Org. Coat.*, 51 (2004) 118.
27. L. Wang, *Corros. Sci.*, 48 (2006) 608.
28. M. Lagrenee, B. Mernari, N. Chaibi, M. Traisnel, H. Vezin and F. Bentiss, *Corros. Sci.*, 43 (2001) 951.
29. S. Rengamani, S. Muralidharan, M. Anbu Kulandainathan and S. Venkatakrishna Iyer, *J. Electrochem. Soc.*, 24 (1994) 355.
30. F. Bentiss, F. Gassama, D. Barbry, L. Gengembre, H. Vezin, M. Lagrenee, M. Traisnel, *Appl. Surf. Sci.*, 252 (2006) 2684.
31. H. Zarrok, R. Saddik, H. Oudda, B. Hammouti, A. El Midaoui, A. Zarrouk, N. Benchat, M. Ebn Touhami, *Der Pharma Chemica.*, 3 (2011) 272.
32. Essassi, E.M.; Lavergne, J.P.; Viallefont, P.; Daunis, J. Recherches en série triazepine-1,2,4:1-détermination de la structure de la triazolotriazépinone obtenue par action de l'acétylacétate d'éthyle sur le diamino-3,4 triazole-1,2,4. *J. Heterocycl. Chem.* **1975**, 12, 661–663.
33. G. Gunasekaran, L.R. Chauhan, *Electrochim. Acta* 49 (2004) 4387.
34. G. Lyberatos, L. Kobotiatis, *Corrosion* 47 (1991) 820.
35. M.S. Abd El Aali, S. Radwan, A. El Saied, *Br. Corros. J.* 18 (1983) 102.
36. A.G. Gad Allah, M.W. Badawy, H.H. Rehan, M.M. Abou-Romia, *J. Appl. Electrochem.* 39 (1989) 928.
37. C. Cao, On electrochemical techniques for interface inhibitor research, *Corros.Sci.* 38 (1996) 2073–2082.

38. H. Vaidyanathan, H. Hackermann, Effect of furan derivatives on the anodic dissolution of Fe, *Corros. Sci.* 11 (1971) 737–750.
39. X. Li, S. Deng, G. Mu, H. Fu, F. Yang, Inhibition effect of nonionic surfactant on the corrosion of cold rolled steel in hydrochloric acid, *Corros. Sci.* 50 (2008) 420–430.
40. M. Behpour, S.M. Ghoreishi, N. Mohammadi, N. Soltani, M. Salavati Niasari, Investigation some Schiff base compounds containing disulfide bond as HCl corrosion inhibitors for mild steel, *Corros. Sci.* 52 (2010) 4046–4057 .
41. M. Belkhaouda, L. Bammou, A. Zarrouk, R. Salghi, E. E. Ebenso, H. Zarrok, B. Hammouti, L. Bazzi , I. Warad. *Int. J. Electrochem. Sci.*, 8 (2013) 7425 – 7436.
42. M. Znini, L. Majidi, A. Bouyanzer, J. Paolini, J.-M. Desjobert , J. Costa, B. Hammouti. *Arabian Journal of Chemistry.* 5 (2012) 467.
43. N. Soltani, N. Tavakkoli, M. Khayatkashani, M. R. Jalali, A. Mosavizade, *Corros. Sci.* 62 (2012) 122.
44. D.A. Lopez, S.N. Simison, S.R. de Sanchez, *Electrochim. Acta* 48 (2003) 845–854.
45. Bentiss, F., Traisnel, M., Lagrenee, M., 2000. The substituted 1,3,4-oxadiazoles: a new class of corrosion inhibitors of mild steel in acidic media. *Corros. Sci.* 42, 127–146.
46. Xianghong Li, Shuduan Deng, Hui Fu, *Corros. Sci.* 62 (2012) 163.
47. A. Popova, E. Sokolova, S. Raicheva, M. Christov, *Corros. Sci.* 45 (2003) 33–58.
48. F.B. Growcock, J.H. Jasinski, *J. Electrochem. Soc.* 136 (1989) 2310–2314.
49. Ehteram A. Noor, Aisha H. Al-Moubaraki, *Mater. Chem. Phys.* 110 (2008) 145.
50. R. Solmaz, G. Kardas, M. Culh, B. Yazici, M. Erbil, *Electrochim. Acta.* 53 (2008) 5941.
51. B. A. Abd-El-Nabey, E. Khamis, M. Sh. Ramadan, A. El-Gindy, *Corrosion (TX)* 52 (1996) 671.
52. H. Ashassi-Sorkhabi, B. Shaabani, D. Seifzadeh, *Appl. Surf. Sci.* 239 (2005) 154.
53. M. M. Osman, R. A. El-Ghazawy, A. M. Al-Sabagh, *Mater. Chem. Phys.* 80 (2003) 55.
54. S. S. Abd El-Rahim, S. A. M Refaey, F. Taha, M. B Saleh, R. A. Ahmed, *J. Appl. Electrochem.* 31 (2001) 429.
55. I. El Ouali, B. Hammouti, A. Aouniti, Y. Ramli, M. Azougagh, E.M. Essassi, M. Bouachrine, *J. Mater. Environ. Sci.*, 2010, 1 (1), 1-8.
56. L. Afia, R. Salghi, L. Bazzi, M. Errami, O. Jbara, S.S. Al-Deyab, B. Hammouti, *Int J Electrochem.Sci.* 6 (2011) 5918.
57. S.S. Abd El Rehim, H.H. Hassan, M.A. Amin, *Mater. Chem. Phys.*, 2001, 70 (1), 64-72
58. E. Sadeghi Meresht, T. Shahrabi Farahani, *J. Neshati, Corros. Sci.* 54 (2012) 36.
59. X.H. Li, S.D. Deng, H. Fu, G.N. Mu, *Corros. Sci.* 51 (2009) 620.
60. R. Fuchs-Godec, V. Dolec ěek, *Colloids Surf. A* 244 (2004) 73.
61. E. Machnikova, K. H. Whitmire, N. Hackerman, *Electrochim. Acta.* 53 (2008) 6024-6032.
62. Z. Szlarska-Smialowska, *Corros. Sci.* 18 (1978) 953–960.
63. A. Yurt, S. Ulutas, H. Dal, *Appl. Surf. Sci.* 253 (2006) 919–925.
64. E. McCafferty, N. Hackerman, *J. Electrochem. Soc.* 119 (1972) 146.
65. Frisch M J, Trucks G W and Schlegel H B *et al.* Gaussian 03, Gaussian, Inc.: Pittsburgh PA, 2003.
66. N. K. Allam, *Appl. Surf. Sci.* 253 (2007) 4570.
67. Lashkari M and Arshadi M R., *Chem Phys*, 2004; 299: 131-137.
68. N. Khalil, *Electrochim. Acta*, 48 (2003) 2635.

(2015); <http://www.jmaterenvironsci.com>